*Computers, Materials & Continua*
DOI: 10.32604/cmc.2023.033705
***Article***



# Sparrow Search Optimization with Transfer Learning-Based Crowd Density Classification

**Mohammad Yamin[1,*], Mishaal Mofleh Almutairi[2], Saeed Badghish[3] and Saleh Bajaba[4]**

[1]Department of Management Information Systems, Faculty of Economics and Administration, King Abdulaziz University, Jeddah, 21589, Saudi Arabia
[2]School of Math, Comp. Sc. and Engg, Department of Electrical and Electronic Engg., London, UK
[3]Department of Marketing, Faculty of Economics and Administration, King Abdulaziz University, Jeddah, 21589, Saudi Arabia
[4]Department of Business Administration, Faculty of Economics and Administration, King Abdulaziz University, Jeddah, 21589, Saudi Arabia
*Corresponding Author: Mohammad Yamin. Email: myamin@kau.edu.sa
Received: 25 June 2022; Accepted: 15 September 2022

**Abstract:** Due to the rapid increase in urbanization and population, crowd gatherings are frequently observed in the form of concerts, political, and religious meetings. HAJJ is one of the well-known crowding events that takes place every year in Makkah, Saudi Arabia. Crowd density estimation and crowd monitoring are significant research areas in Artificial Intelligence (AI) applications. The current research study develops a new Sparrow Search Optimization with Deep Transfer Learning based Crowd Density Detection and Classification (SSODTL-CD2C) model. The presented SSODTL-CD2C technique majorly focuses on the identification and classification of crowd densities. To attain this, SSODTL-CD2C technique exploits Oppositional Salp Swarm Optimization Algorithm (OSSA) with EfficientNet model to derive the feature vectors. At the same time, Stacked Sparse Auto Encoder (SSAE) model is utilized for the classification of crowd densities. Finally, SSO algorithm is employed for optimal fine-tuning of the parameters involved in SSAE mechanism. The performance of the proposed SSODTL-CD2C technique was validated using a dataset with four different kinds of crowd densities. The obtained results demonstrated that the proposed SSODTL-CD2C methodology accomplished an excellent crowd classification performance with a maximum accuracy of 93.25%. So, the proposed method will be highly helpful in managing HAJJ and other crowded events.

**Keywords:** Crowd management; crowd density classification; artificial intelligence; deep learning; computer vision

## 1 Introduction

Automatic examination of severely-congested and distinct varieties of crowded scenes is a difficult task to accomplish due to which the domain has received significant interest among image processing

and computer vision communities. The exponential rise in the global population in recent times, especially in urban regions, paved the way for highly-congested crowds. This unprecedented growth in crowd gatherings poses serious public safety and health issues [1]. Crowd examination and monitoring is a vital processes in public areas in order to provide a safe environment to the public. In recent years, various crowd disasters have occurred owing to the absence of crowd control management. Although crowds comprise of separate individuals, everyone has their own aims and behavioral patterns. The nature of the crowds and their distinct features are commonly interpreted to get cooperative characteristics that can be commonly defined [2,3]. Crowd data like density and flow are vital factors in handling, designing, and managing public places such as political gatherings, temples, etc. [4]. In recent times, the crowd examination domain has concentrated on the development of task-oriented systems that carry out processes like crowd density estimation, crowd counting, anomaly detection, etc. It is reported that the learning of correlated processes, concurrently, can enhance separate task efficiency [5,6].

The existing mass density estimation algorithm [7] that depends upon regression is not precise for 20–50 people gatherings. In certain outdoor scenes like streets and flyovers, crowd density should be mastered. The algorithm can offer data on abnormal crowd flow and crowd distribution on a timely basis [8]. Crowd density assessment, for sparse scenes, is a significant topic and is challenging to accomplish. A Convolution Neural Network (CNN) is nothing but a plain Neural Network (NN) but consists of receptive fields or neurons that possess learnable biases and weights [9]. Every receptive field receives a batch input and implements a convolutional function, after which the outcome is fed into a non-linearity function [10].

Zhu et al. [11] proposed a solution for crowd density estimation problems in sparse or dense conditions. The proposed method has two contributions to the research community; (i) Classification Activation Map (CAM) approach is followed that can offer personal place data and guide in the creation of a whole density map from the last phase (ii) and a network termed 'Patch Scale Discriminant Regression Network (PSDR)' can be utilized to validate the model. In order to provide input crowd images, the proposed algorithm separates the images into patches and sends those image patches, of various density levels, to distinct regression systems in order to obtain the equivalent density map. Fitwi et al. [12] examined a new solution that evaluates interpersonal distance between a couple of dynamic human objects, in the region employed with dynamic density, and the crowd with the help of an edge camera.

Saleem et al. [13] presented a computationally economical and fine-tuned ensemble regression-based Machine Learning (ML) approach to estimate the crowd density. The proposed approach extracted various texture-based features like Grey Level Co-occurrence Matrix (GLCM), Local Binary Patterns (LBP), and Histogram Of Gradients (HOG) and structural features like perimeter of the pixels and its location. Ding et al. [14] examined a new encoding-decoding CNN that combines the feature map with either encoder or decoder sub-networks to generate a further reasonable density map and estimate the count of people accurately. The proposed model has the ability to establish a novel estimation approach called Patch Absolute Error (PAE) which can measure the accuracy of the density maps. In literature [15], a novel testing process was proposed based on the Features from the Accelerated Segment Test (FAST) technique to detect the crowd features using aerial images captured from different camera locations and directions.

Though HAJJ is a regular and well-organized event, thousands of people perished in HAJJ stampedes too, like other crowded events. Indeed, crowded event managers around the globe are continuously looking for technology-driven improved management of crowded events. HAJJ normally

attracts about 2.5 million pilgrims to Makkah, Saudi Arabia. It also comprises of a set of highly complex rituals that require *en masse* participation of all the pilgrims in tight deadlines. For example, all the pilgrims are required to travel from Makkah to Arafat valley which is about 20 km away, and return on the same day. It is extremely challenging to organize transportation facilities for 2.5 million people, for the upward and downward journeys on the same day. Further, all the pilgrims are expected to take part in some other similar activities on the same day or in daylight period. Hectic activities and frequent movement of people *en masse* caused stampedes and other hazards, historically. So, the current research work outcomes will be highly helpful in addressing some of the issues faced by HAJJ pilgrims and participants of other such crowded events. More information on HAJJ and related issues can be found in literature.

The current research study develops a new Sparrow Search Optimization with Deep Transfer Learning based Crowd Density Detection and Classification (SSODTL-CD2C) methodology. The presented SSODTL-CD2C technique exploits the Oppositional Salp Swarm Optimization algorithm (OSSA) with EfficientNet model to derive the feature vectors. At the same time, Stacked Sparse Auto Encoder (SSAE) model is utilized for the classification of crowd densities. Finally, the SSO algorithm is employed for optimal fine-tuning of the parameters involved in the SSAE mechanism. The performance of the proposed SSODTL-CD2C system was validated using a dataset with four different kinds of crowd densities. In short, the contributions of the current study are summarized herewith.

- An intelligent SSODTL-CD2C model consisting of EfficientNet, OSSA-based hyperparameter tuning, and SSO with SSAE classification is presented. To the best of the authors' knowledge, no studies published earlier presented SSODTL-CD2C model
- A novel OSSA-based hyperparameter selection technique is introduced in this study by integrating the concepts of OBL and SSA.
- SSO algorithm is used to optimize the parameters involved in SSAE model using cross-validation. This process helps in increasing the predictive outcomes of the proposed model for unseen data.

## 2 The Proposed Model

In this study, a novel SSODTL-CD2C methodology has been proposed for the identification and classification of crowd densities. Primarily, the proposed SSODTL-CD2C approach exploits OSSA with EfficientNet model to derive the feature vectors. Followed by, SSAE mechanism is utilized for the classification of crowd densities. Eventually, SSO mechanism is employed for optimal fine-tuning of the parameters related to SSAE model. Fig. 1 demonstrates the overall processes involved in SSODTL-CD2C approach.

### *2.1 Feature Extraction*

In this stage, the presented SSODTL-CD2C technique exploits EfficientNet model to derive the feature vectors. EfficientNet is a novel scaling methodology that was recently launched by Google team [16] to scale-up the CNN outcomes. It employs simple and highly-efficient compound coefficients. EfficientNet works differently compared to conventional techniques and scale-up the dimensions of the network including resolution, width, and depth. Further, it also scales up all the dimensions in the network data, using a certain set of scaling coefficients. Practically, the efficiency of the module can be enhanced by scaling up single dimensions. However, balancing each dimension of the network, in terms of accessible resources, increases the whole efficiency of the process. The efficiency of the

scaled-up model strongly depends upon the standard network. It is constructed through AutoML architecture that in turn enhances the effectiveness and precision for the implementation of a neural structure search. Like MnasNet and MobileNetV2, EfficientNet employs mobile inverted bottleneck convolution (MBConv) as its key component. In addition, this system also employs a novel activation function named 'swish' rather than Rectified Linear Unit (ReLU) function. Here, the baseline structure of EfficientNet-B0 and its deep version i.e., EfficientNet-B3 are presented.

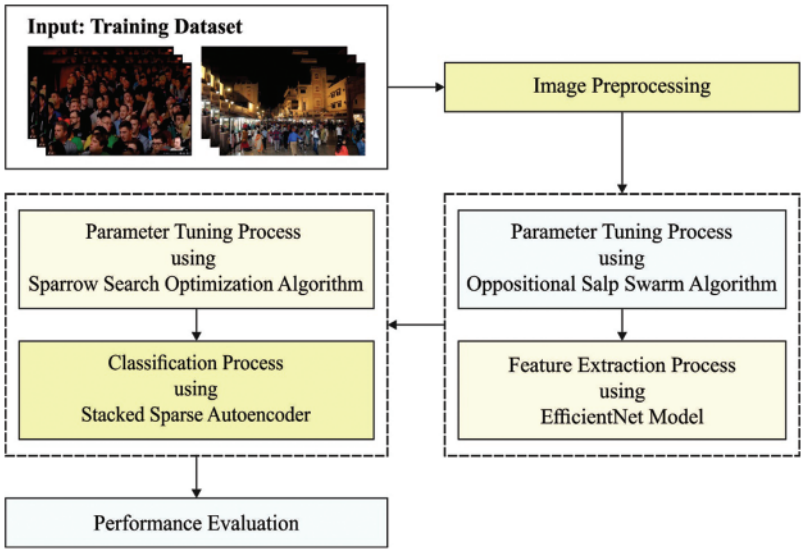


**Figure 1:** The overall process of SSODTL-CD2C approach

### *2.2 Hyperparameter Tuning Using OSSA*

For optimal fine-tuning of the parameters involved in EfficientNet architecture, OSSA is utilized. SSA simulates the swarming performance of Salps. With a transparent body, SSA is simulated by the activities of Salp Swarming in water. Salp swarm is nothing but a chain of salps that use this formation for locomotion during foraging process [17]. For the purpose of modelling the Salps mathematically, the population is separated into two groups such as the leader that lies in front of the chains and its followers i.e., the rest of the salps. In order to update the position of the leader, the subsequent formula is utilized.

$$x_j^1 = \begin{cases} F_j + c_1((ub_j - lb_j)c_2 + lb_j)c_3 \geq 0.5 \\ F_j - c_1((ub_j - lb_j)c_2 + lb_j)c_3 < 0.5 \end{cases} \tag{1}$$

here, $x_j^1$ implies the location of the leader from $j^{th}$ dimension and $ub_j$, $lb_j$ signify the upper and lower bounds of $j^{th}$ dimension correspondingly, $F_j$ implies the place of food sources from $j^{th}$ dimension and $c_1$, $c_2$, and $c_3$ are arbitrarily selected in the interval of 0 and1. In order to achieve a balance between exploration and exploitation, the following control co-efficient $c_1$ is used.

$$c_1 = 2e^{-(\frac{4l}{L})} \tag{2}$$

here, $l$, $L$ refers to the present iteration and the maximal amount of iterations correspondingly. The subsequent formula is established to update the location of the followers. An improved OSSA is derived in this study.

$$x_j^i = \frac{1}{2}\left(x_j^i + x_j^{i-1}\right) \tag{3}$$

The opposite solution is achieved after relating both the solutions. Fig. 2 depicts the flowchart of SSA.


**Figure 2:** Flowchart of SSA

Definition: An opposite number if $x$ is a real number $\in$ [lb, ub], then $\overline{x}$ is provided as follows.

$$\overline{x} = ub + lb - x \tag{4}$$

here, $lb$ refers to lower bound and $ub$ signifies the upper bound of the searching space.

Definition: Opposite Vector, if $x$ refers to multi-dimensional vector, then, $x$ is generalized as follows.

$$\overline{x_j} = ub_j + lb_j - x_j \tag{5}$$

here, $lb_j$, $ub_j$ denote the lower and upper boundaries to $j^{th}$ element of $x$.

### *2.3 Crowd Density Classification Using SSAE Model*

Afterwards, SSAE model is utilized for the classification of crowd densities. Auto Encoder (AE) is an unsupervised learning network structure in which the output and input parameters are similar. Further, the node count in the middle layer is usually lesser than that of the node count on right and left sides. It works with Deep Learning (DL) technique to identify the effective depiction of the input dataset, without any data loss [18]. Briefly, it compresses the new information using encoder to achieve a low dimension that is recreated later into a new information with the help of decoder.

In this algorithm, a trainable encoder can be utilized as a tool to reduce the data dimensionality issues. In comparison with conventional PCA data dimension reduction technique, AE achieves non-linear variations that facilitate the learning of prediction dataset. Even though AE has the ability to accomplish improved data dimensionality reduction compared to other techniques, an AE that is capable of performing dimensionality reduction and increasing the robustness of the data is proposed in this study to adapt for a complex network scenario. Dropout allows every neuron with a probability $p$ to get rejected during network training iteration. Due to this mechanism, every neuron is not reliant completely on other neurons in such a way that the phenomenon of overfitting gets reduced and the generalization capability of a model gets increased to a certain range. By integrating two concepts, a low-latitude representation is attained with the help of dropout and SAE after the reduction of dimensionality. Meanwhile, every dimension has a probability of getting rejected. After dimensionality reduction, the dataset of every dimension is broader than the conventional AE. This phenomenon simplifies the learning process of the model.

Amongst the types of AE, sparse is the most applied type for handling classification problems. In SSAE, all the hidden states are made up of independently-trained SSAEs. Every Stacked Auto Encoder (SAE) considers the output of the hidden state of the preceding SSAE as its own input, so that the features of the input dataset are extracted alongside the hidden layer. This scenario enables the output neuron to implement the classifier after supervised training. Here, the training model is implemented using the above-discussed technique. The presented SSAE structure uses an input layer ($P$ input dataset), two hidden states as output layer ($H$ outputs), and ($M$ and $N$ inputs). This structure is characterized by $P-M-N-H$ SSAE. The study focuses on the implementation of SSAE feedforward stage in which the formula determines the output of *i-th* neuron from *k-th* layer, $z_i^k(n)$, at *n-th* instant as formulated herewith.

$$z_i^k(n) = \sum_{j=1}^{U^l} w_{ij}^k(n) \times y_j^l(n) + wb_i^k(n) \times b \tag{6}$$

In Eq. (6), $w_{ij}^k(n)$ represents the weight of *j-th* input of *i-th* neuron in *k-th* layer at *n-th* instant, $y_j^l(n)$ denotes the *j-th* input of *l-th* layer, in which $l = k-1$, at *n-th* instant, $wb_i^k(n)$ indicates the bias weight of *i-th* neuron from *k-th* layer at *n-th* instant, $b$ represents the bias valued at one whereas $U^l$ denotes the input number of *l-th* layer, in which $U^0 = P$, $U^1 = MeU^2 = N$. In the hidden layer, sigmoid function is applied, hence the output related to the *i-th* neuron from *k-th* layer at *n-th* instant i.e., $v_i^k(n)$, is formulated using the following equation.

$$v_i^k(n) = \left(\frac{1}{1 + e^{-z_i^k(n)}}\right) \tag{7}$$

Here, $v_i^k(n)$ represents the value of *j-th* input that is utilized in the following layer at *n-th* instant i.e., $y_j^{l+1}(n)$ as follows.

$$y_j^{l+1}(n) = v_i^k(n) \tag{8}$$

Now $j = i$. The *softmax* activation function is utilized in the output neuron. This function is adapted in neural classifier network as given below.

$$s_i(n) = \frac{e^{z_i^K(n)}}{\sum_{h=1}^{H} e^{z_h^K(n)}} \tag{9}$$

here, $s_i(n)$ comprises of *i-th* output of $K$ final layer with $H$ neuron at *n-th* instant. The $H$ values are described through the class count of the problem since this function characterizes the likelihood that every dataset belongs to a certain class.

### *2.4 Parameter Tuning Using SSO Algorithm*

In this final stage, SSO approach is employed for optimal fine-tuning of the parameters involved in SSAE mechanism. SSO algorithm is an emergent evolutionary mechanism, inspired by anti-predation and sparrow foraging behaviours [19]. In comparison with conventional evolutionary algorithms, SSO algorithm has faster convergence speed and strong global search capability in terms of optimization issues. In SSO algorithm, the population is classified as producer and scrounger groups. At first, the producer group executes a large searching step to search for food. Then, the scrounger group follows the producer to find the food. In this searching method, the scrounger group has a huge probability to search for food through subsequent behaviour. However, the roles played by producer and scrounger are dynamically adjusted to search for high quality food sources. Subsequently, SSO algorithm is mathematically modelled as given herewith.

Step 1: Define the parameters such as maximum iteration ($g_{\max}$), sparrow count (N), number of producers ($PN$) and scroungers (N-PN). The position of the *i-th* sparrow is determined by $x_i = (x_{i,1}, x_{i,2}, \ldots, x_{i,D})$ whereas $f(x_i)$ denotes the fitness value of *i-th* sparrow. Next, the initialized swarm $x$ is formulated as given herewith [20].

$$x = \begin{Bmatrix} x_{1,1} & \cdots & x_{1,d} \\ \vdots & x_{i,j} & \vdots \\ x_{N,1} & \ldots & x_{N,D} \end{Bmatrix} \tag{10}$$

In Eq. (10), $x_{i,j}$ represents the *j-th* element value of *i-th* sparrow. $D$ indicates the decision variable count.

Step 2: The position of the producer is upgraded as given herewith.

$$x_i^{g+1} = \begin{cases} x_i^g \cdot \exp\left[\frac{-i}{\alpha \cdot g_{\max}}\right] & if\,(R < ST) \\ x_i^g + Q \cdot L & else\ i \in [1, PN], \end{cases} \tag{11}$$

In Eq. (11), $g$ denotes the iterative index; $a$ represents a random integer between [0,1]; $Q$ denotes a uniformly-distributed random number; $L$ indicates a $1 \times D$ matrix in which the element is fixed at one. $R \in [0, 1]$ and $ST \in [0.5, 1.0]$ signify the alarm value and safety thresholding value correspondingly. $R < ST$ i.e., the producer implements the general searching mode without the influence of the predator; In $R \geq ST$, the predator is found by the sparrow and each sparrow must fly towards the safest region [21].

Step 3: The position of the scrounger is upgraded as follows.

$$x_i^{g+1} = \begin{cases} Q.\exp\left[\frac{G_{worst} - x_i^g}{i^2}\right] & if\,(i > N/2) \\ S_{best} + |x_i^g - S_{best}| \cdot A^+ \cdot L & else\ i \in [PN + 1, N], \end{cases} \tag{12}$$

In Eq. (12), $S_{best}$ represents the well-known position of the producer; $G_{Worst}$ indicates the global worst known position identified; $A$ symbolizes a $1 \times D$ matrix while each component is arbitrarily chosen in the range of $\{1, -1\}$; as well as $A^+ = A^T(AA^T)^{-1}$. If $i > N/2$, the *i-th* scrounger must find another area to search for energy; or else, *i-th* scrounger is foraged in the region nearby $S_{best}$.

Step 4: In order to prevent potential danger, around 10–20 per cent of sparrows in the swarm are designated at a random fashion as scouters and their positions are upgraded as follows.

$$x_i^{g+1} = \begin{cases} G_{best} + \beta \cdot |x_i^g - G_{best}| & if(f(x_i^g) > f(G_{worst})) \\ x_i^g + \frac{K \cdot |x_i^g - G_{worst}|}{f(x_i^g) + f(G_{worst}) + \theta} & if(f(x_i^g) = f(G_{worst})) \end{cases} \tag{13}$$

In Eq. (13), $\beta$ represents a random number that obeys uniform distribution; $G_{best}$ indicates the global well known position; $K \in [-1, 1]$ denotes an arbitrary integer which illustrates the searching step size and $\theta$ indicates a smaller constant that is utilized to avoid the denominator being 0. Here, $(x_i^g) > f(G_{worst})$, the *i-th* sparrow at the edge of the swarm gets easily identified by the predators; or else, the *i-th* sparrow at the centre of the swarm must be closer to another sparrow for anti-predation.

Step 5: Upgrade the best and worst fitness values to obtain the novel position of each sparrow.

Step 6: When the end criteria are not satisfied, proceed to Step 2 for the following cycle; or else, the global better known location is found through sparrow population and is processed as the final solution for the targeted problem.

## 3 Experimental Validation

In this section, the crowd classification performance of the proposed SSODTL-CD2C method was validated using a dataset of 2,000 samples under four classes. Each class holds a set of 500 samples. Since no benchmark dataset is available in the literature, the current study authors have collected their own dataset. Table 1 depicts the details of the datasets.

**Table 1:** Dataset details

| Labels | Description | No. of samples |
|---|---|---|
| Class1 | Dense crowd | 500 |
| Class2 | Medium dense crowd | 500 |
| Class3 | Sparse crowd | 500 |
| Class4 | No crowd | 500 |
| Total No. of samples | | 2000 |

Fig. 3 reports the confusion matrices generated by the proposed SSODTL-CD2C model with 70:30 of TR/TS datasets. With 70% of training (TR) data, the proposed SSODTL-CD2C model recognized 270 samples as class 1, 244 samples as class 2, 313 samples as class 3 and 309 samples as class 4. Moreover, in 30% of testing (TS) dataset, the presented SSODTL-CD2C method classified 122 samples under class 1, 121 samples under class 2, 119 samples under class 3, and 139 samples under class 4.

Table 2 provides the overall crowd classification outcomes achieved by the proposed SSODTL-CD2C method on 70:30 of TR/TS datasets.

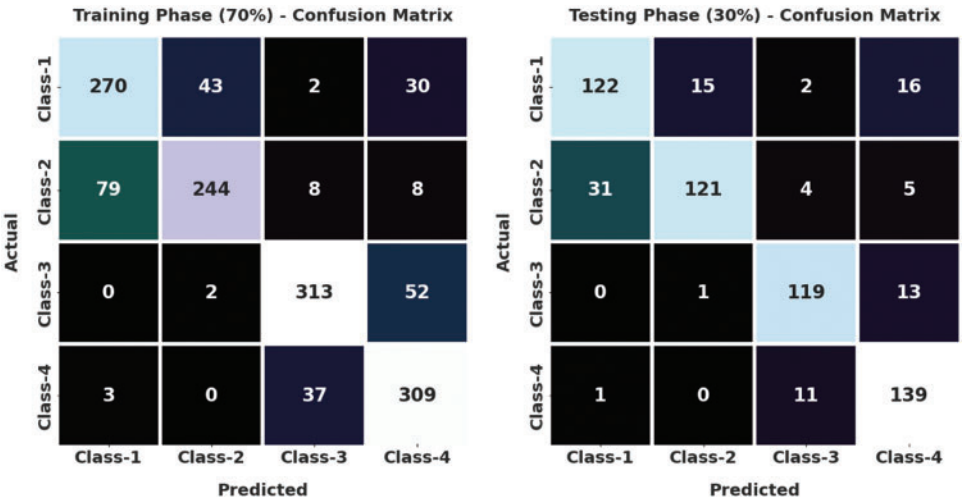


**Figure 3:** Confusion matrices of SSODTL-CD2C approach (a) 70% of TR data and (b) 30% of TS data

**Table 2:** Results of the analysis of SSODTL-CD2C methodology on 70:30 of TR/TS datasets under different measures

| Labels | Accuracy | Precision | Recall | F-Score | G-Mean |
|---|---|---|---|---|---|
| Training phase (70%) | | | | | |
| Class-1 | 88.79 | 76.70 | 78.26 | 77.47 | 84.96 |
| Class-2 | 90.00 | 84.43 | 71.98 | 77.71 | 83.02 |
| Class-3 | 92.79 | 86.94 | 85.29 | 86.11 | 90.23 |
| Class-4 | 90.71 | 77.44 | 88.54 | 82.62 | 89.98 |
| Average | 90.57 | 81.38 | 81.02 | 80.98 | 87.04 |
| Testing phase (30%) | | | | | |
| Class-1 | 89.17 | 79.22 | 78.71 | 78.96 | 85.47 |
| Class-2 | 90.67 | 88.32 | 75.16 | 81.21 | 85.10 |
| Class-3 | 94.83 | 87.50 | 89.47 | 88.48 | 92.85 |
| Class-4 | 92.33 | 80.35 | 92.05 | 85.80 | 92.24 |
| Average | 91.75 | 83.85 | 83.85 | 83.61 | 88.91 |

Fig. 4 exhibits the classification performance of the presented SSODTL-CD2C method on 70% of TR data. The figure shows that SSODTL-CD2C technique obtained effective outcomes under all the classes. For example, in class 1, the presented SSODTL-CD2C approach reached an $accu_y$ of 88.79%, $prec_n$ of 76.70%, $reca_l$ of 78.26%, $F_{score}$ of 77.47%, and a $G_{mean}$ of 84.96%. Eventually, in class 3, the proposed SSODTL-CD2C method obtained an $accu_y$ of 92.79%, $prec_n$ of 86.94%, $reca_l$ of 85.29%,

$F_{score}$ of 86.11%, and a $G_{mean}$ of 90.23%. Meanwhile, in class 4, the presented SSODTL-CD2C approach attained an $accu_y$ of 90.71%, $prec_n$ of 77.44%, $reca_l$ of 88.54%, $F_{score}$ of 82.62%, and a $G_{mean}$ of 89.98%.

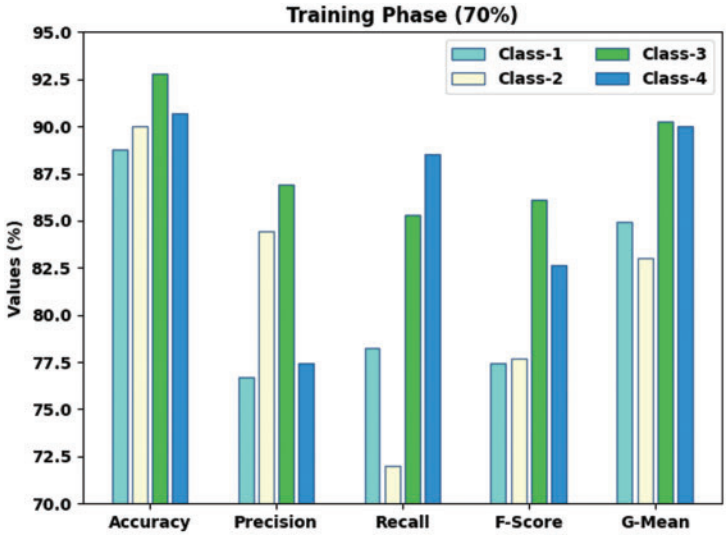


**Figure 4:** Results of the analysis of SSODTL-CD2C method under 70% of TR dataset

Fig. 5 displays the classification performance of the proposed SSODTL-CD2C approach on 30% of TS data. The figure shows that the presented SSODTL-CD2C approach achieved effective results under each class. For example, in class 1, the proposed SSODTL-CD2C method attained an $accu_y$ of 89.17%, $prec_n$ of 79.22%, $reca_l$ of 78.71%, $F_{score}$ of 78.96%, and a $G_{mean}$ of 85.47%. Eventually, in class 3, the proposed SSODTL-CD2C technique attained an $accu_y$ of 94.83%, $prec_n$ of 87.50%, $reca_l$ of 89.47%, $F_{score}$ of 88.48%, and a $G_{mean}$ of 92.85%. Meanwhile, in class 4, the proposed SSODTL-CD2C system obtained an $accu_y$ of 92.33%, $prec_n$ of 80.35%, $reca_l$ of 92.05%, $F_{score}$ of 85.80%, and a $G_{mean}$ of 92.24%.

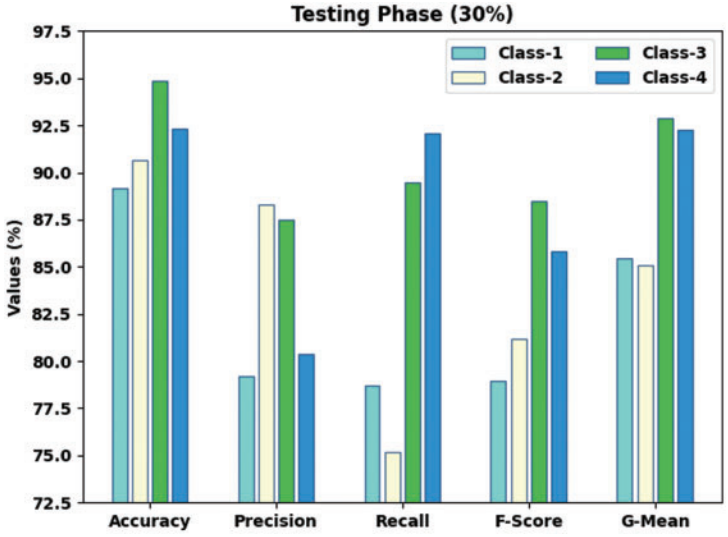


**Figure 5:** Results of the analysis of SSODTL-CD2C system under 30% of TS dataset

Fig. 6 demonstrates the confusion matrices generated by the proposed SSODTL-CD2C method with 80:20 of TR/TS datasets. With 80% of TR data, SSODTL-CD2C technique recognized 325 samples under class 1, 388 samples under class 2, 368 samples under class 3, and 342 samples under class 4. Furthermore, in 20% of TS data, the presented SSODTL-CD2C approach categorized 93 samples under class 1, 87 samples under class 2, 82 samples under class 3, and 84 samples under class 4.

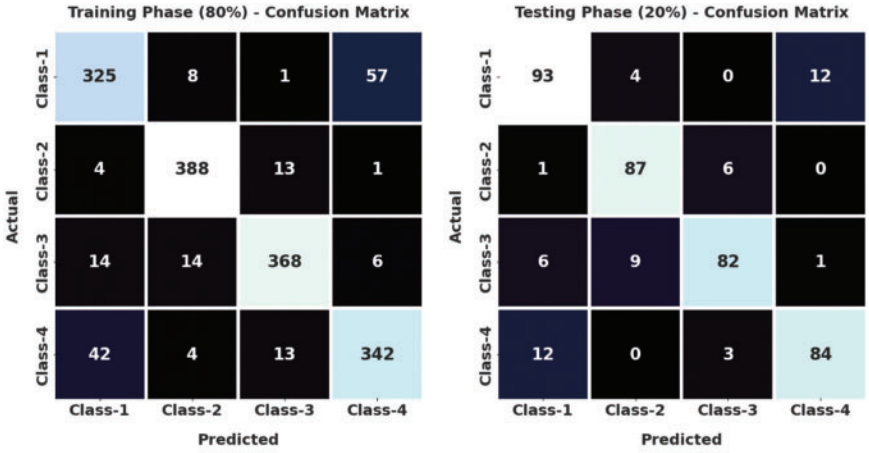


(a) (b)

**Figure 6:** Confusion matrices of SSODTL-CD2C approach (a) 80% of TR data and (b) 20% of TS data

Table 3 offers the overall crowd classification results accomplished by the proposed SSODTL-CD2C method on 80:20 of TR/TS datasets.

**Table 3:** Results of the analysis of SSODTL-CD2C methodology on 80:20 of TR/TS datasets under different measures

| Labels | Accuracy | Precision | Recall | F-Score | G-Mean |
|---|---|---|---|---|---|
| Training phase (80%) | | | | | |
| Class-1 | 92.13 | 84.42 | 83.12 | 83.76 | 88.88 |
| Class-2 | 97.25 | 93.72 | 95.57 | 94.63 | 96.69 |
| Class-3 | 96.19 | 93.16 | 91.54 | 92.35 | 94.59 |
| Class-4 | 92.31 | 84.24 | 85.29 | 84.76 | 89.85 |
| Average | 94.47 | 88.88 | 88.88 | 88.88 | 92.50 |
| Testing phase (20%) | | | | | |
| Class-1 | 91.25 | 83.04 | 85.32 | 84.16 | 89.30 |
| Class-2 | 95.00 | 87.00 | 92.55 | 89.69 | 94.14 |
| Class-3 | 93.75 | 90.11 | 83.67 | 86.77 | 90.10 |
| Class-4 | 93.00 | 86.60 | 84.85 | 85.71 | 90.10 |
| Average | 93.25 | 86.69 | 86.60 | 86.59 | 90.91 |

Fig. 7 demonstrates the classification performance of the presented SSODTL-CD2C method on 80% of TR data. The figure shows that SSODTL-CD2C method attained effective results under each class. For example, in class 1, the proposed SSODTL-CD2C technique produced an $accu_y$ of 92.13%, $prec_n$ of 84.42%, $reca_l$ of 83.12%, $F_{score}$ of 83.76%, and a $G_{mean}$ of 88.88%. Eventually, in class 3, SSODTL-CD2C technique obtained an $accu_y$ of 96.19%, $prec_n$ of 93.16%, $reca_l$ of 91.54%, $F_{score}$ of 92.35%, and a $G_{mean}$ of 94.59%. Meanwhile, in class 4, the proposed SSODTL-CD2C approach attained an $accu_y$ of 92.31%, $prec_n$ of 84.24%, $reca_l$ of 85.29%, $F_{score}$ of 84.76%, and a $G_{mean}$ of 89.85%.

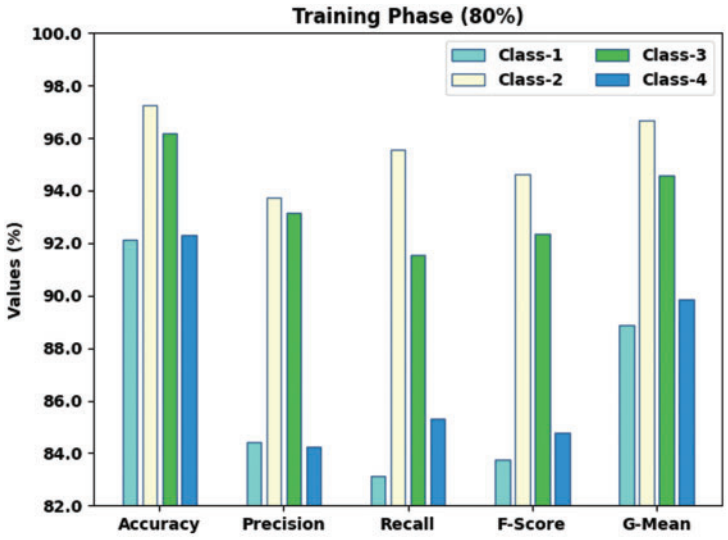


**Figure 7:** Results of the analysis of SSODTL-CD2C methodology under 80% of TR dataset

Fig. 8 displays the classification performance achieved by the proposed SSODTL-CD2C system on 20% of TS dataset. The figure shows that SSODTL-CD2C technique attained effective results under each class. For example, in class 1, the proposed SSODTL-CD2C method attained an $accu_y$ of 91.25%, $prec_n$ of 83.04%, $reca_l$ of 85.32%, $F_{score}$ of 84.16%, and a $G_{mean}$ of 89.30%. Eventually, in class 3, the proposed SSODTL-CD2C method attained an $accu_y$ of 93.75%, $prec_n$ of 90.11%, $reca_l$ of 83.67%, $F_{score}$ of 86.77%, and a $G_{mean}$ of 90.10%. Meanwhile, in class 4, the proposed SSODTL-CD2C approach attained an $accu_y$ of 93%, $prec_n$ of 86.60%, $reca_l$ of 84.85%, $F_{score}$ of 85.71%, and a $G_{mean}$ of 90.10%.

Both Training Accuracy (TA) and Validation Accuracy (VA) values, achieved by the proposed SSODTL-CD2C methodology on testing data, are illustrated in Fig. 9. The experimental result indicate that the proposed SSODTL-CD2C approach accomplished the maximal TA and VA values while VA values were higher than TA.

Both Training Loss (TL) and Validation Loss (VL) values, accomplished by the proposed SSODTL-CD2C methodology on testing data, are demonstrated in Fig. 10. The experimental outcomes infer that the proposed SSODTL-CD2C approach obtained minimal TL and VL values whereas VL values were lower than TL.

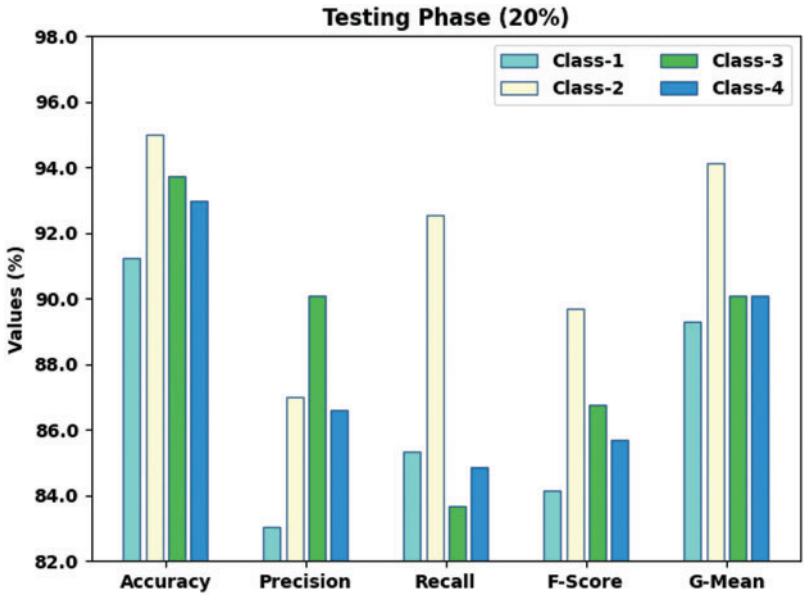


**Figure 8:** Results of the analysis of SSODTL-CD2C method under 20% of TS dataset

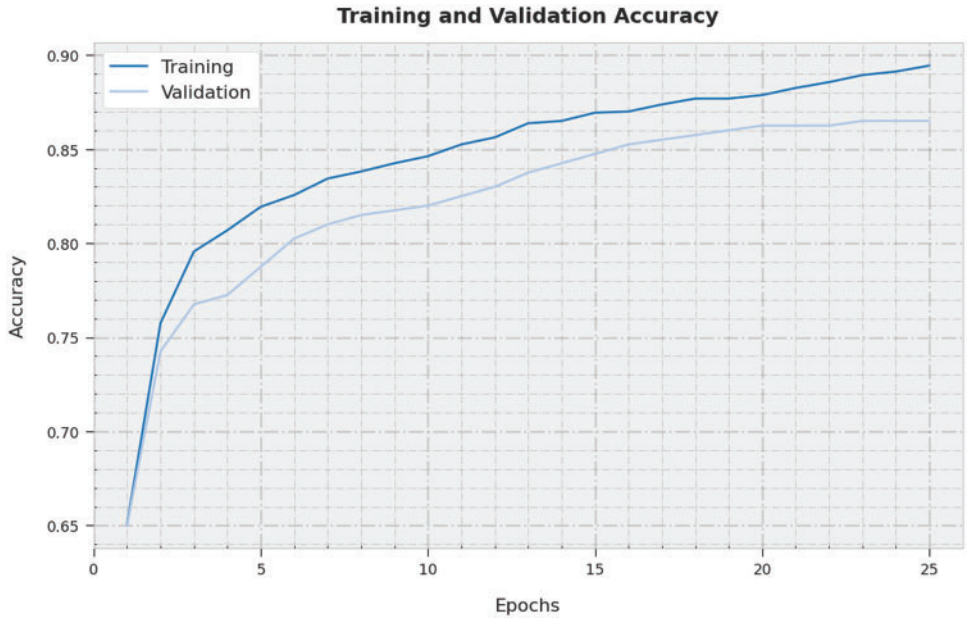


**Figure 9:** TA and VA analyses results of SSODTL-CD2C methodology

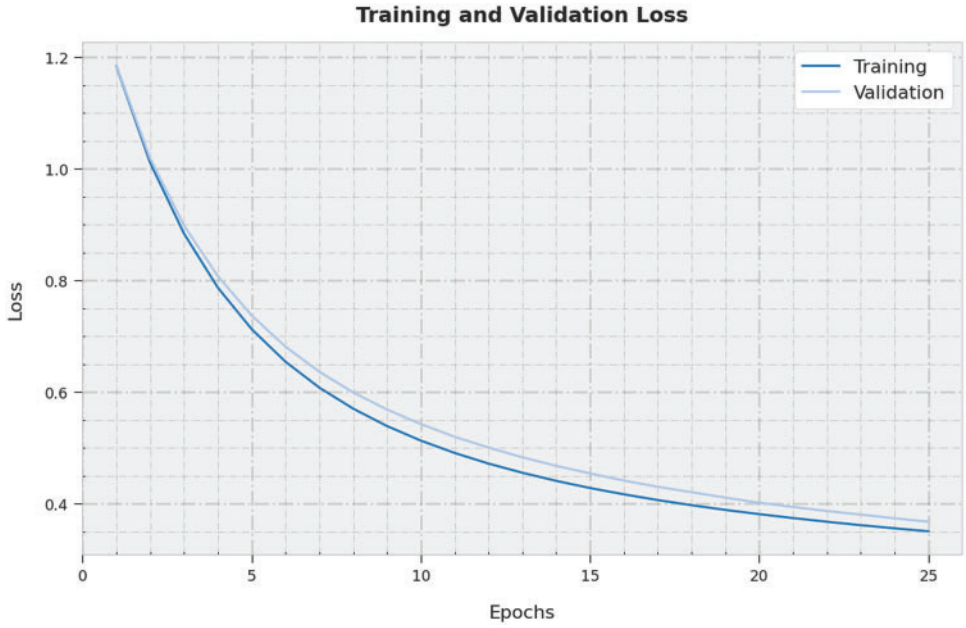


**Figure 10:** TL and VL analyses results of SSODTL-CD2C method

A clear precision-recall examination was conducted upon SSODTL-CD2C system using testing dataset and the results are shown in Fig. 11. The figure specifies that the proposed SSODTL-CD2C process produced improved precision-recall values under each class.

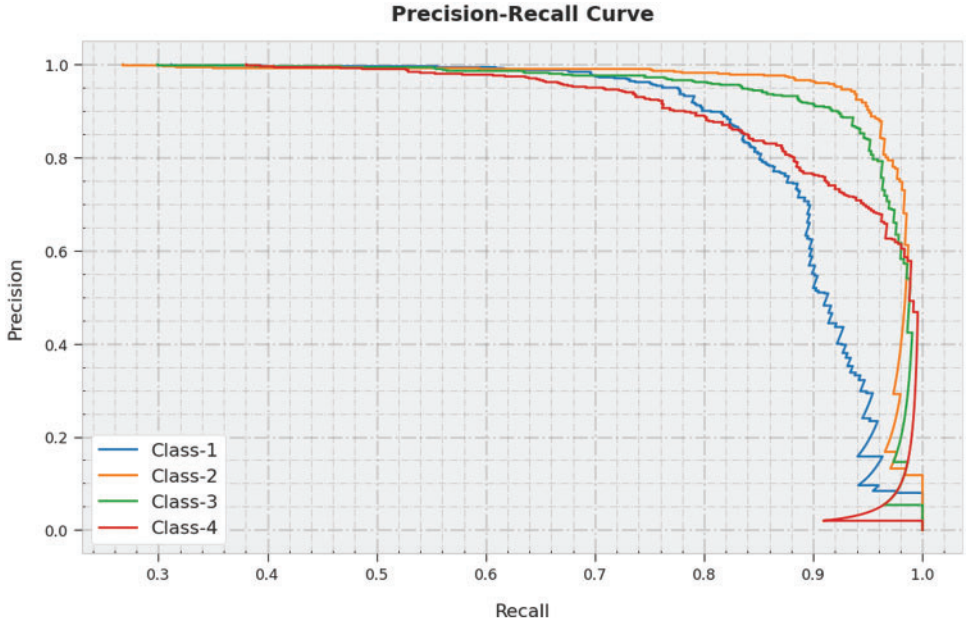


**Figure 11:** Precision-recall curve analysis results of SSODTL-CD2C methodology

A brief Receiver Operating Characteristic (ROC) analysis was conducted upon SSODTL-CD2C methodology on testing dataset and the results are portrayed in Fig. 12. The results denote that the proposed SSODTL-CD2C method demonstrated its capability in classifying the testing dataset under different classes.

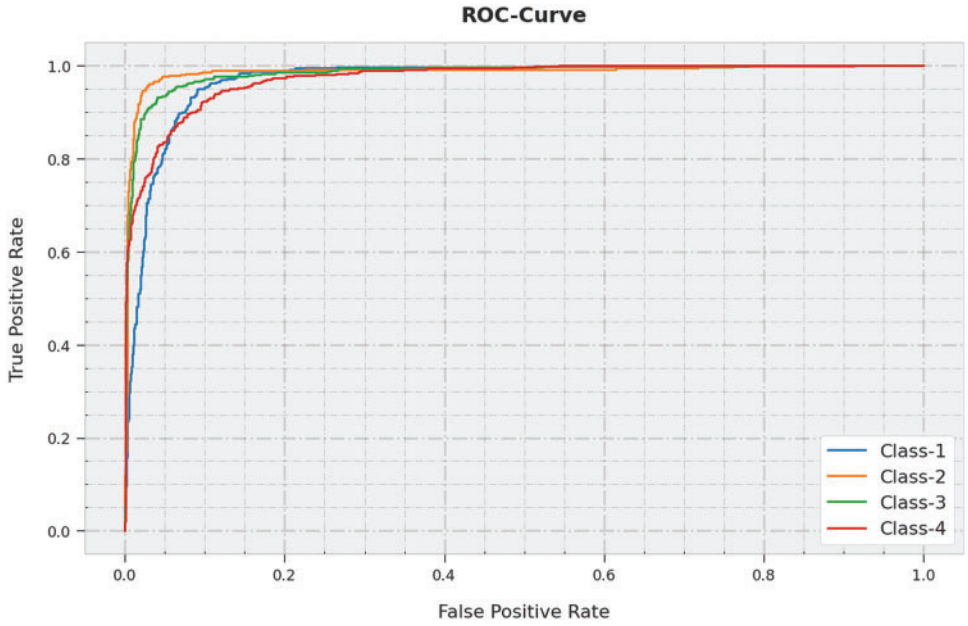


**Figure 12:** ROC curve analysis of SSODTL-CD2C method

To assure the enhanced performance of the proposed SSODTL-CD2C model, a detailed comparative study was conducted and the results are shown in Table 4 [22,23]. The experimental values highlight that the proposed SSODTL-CD2C technique produced high $accu_y$ values over other models, under all classes. For example, in class 1, the proposed SSODTL-CD2C method achieved a high $accu_y$ of 91.25%, whereas Gabor, Bag–of–words with SRP (BoWSRP), BowLBP, GLCM with Support Vector Machine (GLCMSVM), and VGG-Net models reported the least $accu_y$ values such as 55.22%, 80.48%, 90.95%, 72.95%, and 87.20% respectively. Meanwhile, in class 2, the proposed SSODTL-CD2C method achieved increased $accu_y$ values such as 95%, while Gabor, BoWSRP, BowLBP, GLCMSVM, and VGG-Net models produced low $accu_y$ values such as 80.95%, 86.98%, 80.39%, 82.23%, and 82.47% correspondingly. Eventually, in class 3, the proposed SSODTL-CD2C model offered a high $accu_y$ of 93%, whereas Gabor, BoWSRP, BowLBP, GLCMSVM, and VGG-Net models achieved low $accu_y$ values such as 85.64%, 83.82%, 89.16%, 92%, and 90.03% correspondingly.

**Table 4:** Comparative accuracy analysis results of SSODTL-CD2C approach and other recent methods

| Accuracy (%) | | | | | |
|---|---|---|---|---|---|
| Methods | Class 1 | Class 2 | Class 3 | Class 4 | Average |
| Gabor | 55.22 | 80.95 | 66.06 | 85.64 | 71.97 |
| BoWSRP | 80.48 | 86.98 | 71.15 | 83.82 | 80.61 |

(Continued)

**Table 4:** Continued

| | Accuracy (%) | | | | |
|---|---|---|---|---|---|
| BowLBP | 90.95 | 80.39 | 77.28 | 89.16 | 84.45 |
| GLCMSVM | 72.95 | 82.23 | 71.33 | 92.00 | 79.63 |
| VGG-Net | 87.20 | 82.47 | 79.45 | 90.03 | 84.79 |
| SSODTL-CD2C | 91.25 | 95.00 | 93.75 | 93.00 | 93.25 |

## 4 Conclusion

In this study, the SSODTL-CD2C approach has been presented for the identification and classification of crowd densities. Primarily, the SSODTL-CD2C technique exploited the OSSA with EfficientNet model to derive the feature vectors. Followed by, the SSAE model is utilized for the classification of the crowd densities. Eventually, the SSO technique is employed for the optimal fine-tuning of the parameters based on the SSAE method. The performance of the proposed SSODTL-CD2C technique was validated using the dataset with four different kinds of crowd densities. The obtained outcomes inferred the superior performance of SSODTL-CD2C approach with maximal crowd classification performance. As a part of the future scope, a new crowd counting approach should be derived to estimate the number of people. As commented earlier, the current research would help in achieving better crowd management for all the events globally.

**Funding Statement:** This research work was funded by Institutional Fund Projects under grant no. (IFPHI-097-120-2020). Therefore, authors gratefully acknowledge technical and financial support from the Ministry of education and King Abdulaziz University, DSR, Jeddah, Saudi Arabia.

**Conflicts of Interest:** The authors declare that they have no conflicts of interest to report regarding the present study.

## References

[1] G. Sreenu and M. A. S. Durai, "Intelligent video surveillance: A review through deep learning techniques for crowd analysis," *Journal of Big Data*, vol. 6, no. 1, pp. 48, 2019.

[2] L. Chen, G. Wang and G. Hou, "Multi-scale and multi-column convolutional neural network for crowd density estimation," *Multimedia Tools and Applications*, vol. 80, no. 5, pp. 6661–6674, 2021.

[3] H. Zheng, Z. Lin, J. Cen, Z. Wu and Y. Zhao, "Cross-line pedestrian counting based on spatially-consistent two-stage local crowd density estimation and accumulation," *IEEE Transactions on Circuits and Systems for Video Technology*, vol. 29, no. 3, pp. 787–799, 2019.

[4] A. Khan, J. A. Shah, K. Kadir, W. Albattah and F. Khan, "Crowd monitoring and localization using deep convolutional neural network: A review," *Applied Sciences*, vol. 10, no. 14, pp. 4781, 2020.

[5] D. Chaudhary, S. Kumar and V. S. Dhaka, "Video based human crowd analysis using machine learning: A survey," *Computer Methods in Biomechanics and Biomedical Engineering: Imaging & Visualization*, vol. 10, no. 2, pp. 113–131, 2022.

[6] H. Ullah, I. U. Islam, M. Ullah, M. Afaq, S. D. Khan *et al.,* "Multi-feature-based crowd video modeling for visual event detection," *Multimedia Systems*, vol. 27, no. 4, pp. 589–597, 2021.

[7] H. Ammar and A. Cherif, "DeepROD: A deep learning approach for real-time and online detection of a panic behavior in human crowds," *Machine Vision and Applications*, vol. 32, no. 3, pp. 1–15, 2021.

[8] S. Elbishlawi, M. H. Abdelpakey, A. Eltantawy, M. S. Shehata and M. M. Mohamed, "Deep learning-based crowd scene analysis survey," *Journal of Imaging*, vol. 6, no. 9, pp. 95, 2020.

[9] G. Tripathi, K. Singh and D. K. Vishwakarma, "Convolutional neural networks for crowd behaviour analysis: A survey," *The Visual Computer*, vol. 35, no. 5, pp. 753–776, 2019.
[10] H. Jiang and W. Jin, "Effective use of convolutional neural networks and diverse deep supervision for better crowd counting," *Applied Intelligence*, vol. 49, no. 7, pp. 2415–2433, 2019.
[11] L. Zhu, C. Li, Z. Yang, K. Yuan and S. Wang, "Crowd density estimation based on classification activation map and patch density level," *Neural Computing and Applications*, vol. 32, no. 9, pp. 5105–5116, 2020.
[12] A. Fitwi, Y. Chen, H. Sun and R. Harrod, "Estimating interpersonal distance and crowd density with a single-edge camera," *Computers*, vol. 10, no. 11, pp. 143, 2021.
[13] M. S. Saleem, M. J. Khan, K. Khurshid and M. S. Hanif, "Crowd density estimation in still images using multiple local features and boosting regression ensemble," *Neural Computing and Applications*, vol. 32, no. 21, pp. 16445–16454, 2020.
[14] X. Ding, F. He, Z. Lin, Y. Wang, H. Guo *et al.,* "Crowd density estimation using fusion of multi-layer features," *IEEE Transactions on Intelligent Transportation Systems*, vol. 22, no. 8, pp. 4776–4787, 2021.
[15] A. Almagbile, "Estimation of crowd density from UAVs images based on corner detection procedures and clustering analysis," *Geo-spatial Information Science*, vol. 22, no. 1, pp. 23–34, 2019.
[16] Y. Bazi, M. M. Al Rahhal, H. Alhichri and N. Alajlan, "Simple yet effective fine-tuning of deep CNNs using an auxiliary classification loss for remote sensing scene classification," *Remote Sensing*, vol. 11, no. 24, pp. 2908, 2019.
[17] M. Zivkovic, C. Stoean, A. Chhabra, N. Budimirovic, A. Petrovic *et al.,* "Novel improved salp swarm algorithm: An application for feature selection," *Sensors*, vol. 22, no. 5, pp. 1711, 2022.
[18] J. Xu, L. Xiang, Q. Liu, H. Gilmore, J. Wu *et al.,* "Stacked sparse auto encoder (SSAE) for nuclei detection on breast cancer histopathology images," *IEEE Transactions on Medical Imaging*, vol. 35, no. 1, pp. 119–130, 2016.
[19] J. Xue and B. Shen, "A novel swarm intelligence optimization approach: Sparrow search algorithm," *Systems Science & Control Engineering*, vol. 8, no. 1, pp. 22–34, 2020.
[20] Q. Liu, Y. Zhang, M. Li, Z. Zhang, N. Cao *et al.,* "Multi-UAV path planning based on fusion of sparrow search algorithm and improved bioinspired neural network," *IEEE Access*, vol. 9, pp. 124670–124681, 2021.
[21] R. Liu, G. Li, L. Wie, Y. Xu, X. Gou *et al.,* "Spatial prediction of groundwater potentiality using machine learning methods with grey wolf and sparrow search algorithms," *Journal of Hydrology*, vol. 610, pp. 127977, 2022.
[22] O. Meynberg, S. Cui and P. Reinartz, "Detection of high-density crowds in aerial images using texture classification," *Remote Sensing*, vol. 8, no. 6, pp. 470, 2016.
[23] S. Pu, T. Song, Y. Zhang and D. Xie, "Estimation of crowd density in surveillance scenes based on deep convolutional neural network," *Procedia Computer Science*, vol. 111, no. 3, pp. 154–159, 2017.